

Raman Spectroscopy Study of $\text{Zn}_{1-x}\text{Fe}_x\text{Se}$ under High Pressure

Chih-Ming Lin^{1*} and Der-San Chuu²

¹ National Hsinchu Teachers' College, Hsinchu, Taiwan, R.O.C.

² Department of Electro-Physics, National Chiao Tung University, Hsinchu, Taiwan, R.O.C.

$\text{Zn}_{1-x}\text{Fe}_x\text{Se}$, $x = 0, 0.018, 0.035$ and 0.16 , were studied by Raman scattering spectroscopy up to 35.0 GPa. It was found that the semiconductor–metal phase transition pressures for these samples are 14.4, 12.8, 12.0 and 10.9 GPa, respectively. Before the semiconductor–metal phase transition, a visible anomaly of the TO Raman mode splitting was observed at 4.7 and 9.1 GPa for ZnSe, at 3.3 and 5.9 GPa for $\text{Zn}_{0.982}\text{Fe}_{0.018}\text{Se}$, and at 4.5 and 7.2 GPa for $\text{Zn}_{0.965}\text{Fe}_{0.035}\text{Se}$, respectively, while $\text{Zn}_{0.84}\text{Fe}_{0.16}\text{Se}$ showed mode splitting at 4.7 GPa only. For these samples, one of the TO splitting modes exhibits phonon softening (red shift), while the other manifests wavenumber increasing (blue shift) with pressure. For $x = 0.018, 0.035$ and 0.16 , a new Raman mode, which was identified as Fe local mode, was observed between the pure ZnSe LO and TO modes. Fe local mode exhibits blue shift behaviour before metallization and disappears as the pressure is higher beyond the metallization pressure. PACS numbers: 62.50. + *p*, 64.60. – *i*, 78.30.Fs. Copyright © 1999 John Wiley & Sons, Ltd.

INTRODUCTION

$\text{Zn}_{1-x}\text{Fe}_x\text{Se}$ ternary compound crystals represent a giant interesting sub-class of semi-magnetic semiconductors (SMSC),^{1–3} which contain interesting properties of electronic structure, far-IR absorption and Raman scattering spectroscopy, high field magnetization, exchange effects between ions and band carriers, and so on. In the past decade, the high-pressure behaviours of $\text{Zn}_{1-x}\text{Fe}_x\text{Se}$ have attracted much attention since the high-pressure-induced phase transition of the $\text{Zn}_{0.83}\text{Fe}_{0.17}\text{Se}$ crystal was discussed by Qudri *et al.*⁴ by using energy-dispersive x-ray-diffraction (EDXD) measurement. Qudri *et al.* found that the existence of Fe in the crystal results in a reduction in the transition pressure due to hybridization of 3d orbitals into tetrahedral bonds. The role played by Fe in the observation of the reduction in the transition pressure of $\text{Zn}_{1-x}\text{Fe}_x\text{Se}$ is similar to the role that Mn plays in the $\text{Zn}_{1-x}\text{Mn}_x\text{Se}$ ^{5–7} crystal. Lin *et al.*^{8–10} also found by using micro-Raman and EDXD measurements that the $\text{Zn}_{0.84}\text{Fe}_{0.16}\text{Se}$ crystal underwent structural transformation from a four-coordinated B3 structure to a six-coordinated B1 structure under high pressure. For theoretical studies, no report on the phase transformation of $\text{Zn}_{1-x}\text{Fe}_x\text{Se}$ under high pressure has been published. But for ZnSe, Andreoni *et al.* used a soft-core self-consistent pseudopotential plane wave method¹¹ to predict that ZnSe formed a new semiconductor phase at transition pressure. Smelyansky *et al.*¹² showed that the high-pressure phase of ZnSe was metallized by using the full potential linearly augmented plane wave approach and numerical atomic orbital band structure calculations within the local-density

approximation.¹² Smelyansky *et al.*¹² and Itkin *et al.*¹³ suggested that the metallization occurs when ZnSe transforms from a four-coordinated zinc-blende (ZB) phase into a six-coordinated rock salt (RS) phase. Recently, Michel *et al.*¹⁴ reported that ZnSe follows the structural transition sequence: zinc-blende → cinnabar → NaCl → Cmcn with increasing pressure by using the *ab initio* pseudopotential calculation. Similarly, Ahuji *et al.*¹⁵ also indicated that CdTe follows the structural sequence: zinc-blende → cinnabar → NaCl → orthorhombic with increasing pressure by using the full-potential linear muffin-tin-orbital (FPLMTO) calculation in the study of the structural phase transition of CdTe under high pressure. A similar study of the ZB structure of CdTe¹⁶ showed that one more phase exists below the structure transformation from ZB to RS structure.

In this work, Raman scattering measurements were performed to investigate the pressure effect on the phase transition of $\text{Zn}_{1-x}\text{Fe}_x\text{Se}$ crystals with $x = 0, 0.018, 0.035$ and 0.16 , under high pressure up to around 35.0 GPa. It was found that these samples exhibit four phase regions and two unidentified transitions occur respectively at 4.7 and 9.1 GPa, 3.3 and 5.9 GPa, 4.5 and 7.2 GPa, and 4.7 GPa for $x = 0, 0.018, 0.035$ and 0.16 . In addition, three split transverse optical (TO) phonon modes can be observed for pressure even higher than the metallization pressure. These split TO modes are found to persist up to 35.0 GPa. The effect of the Fe element on the phase transition will also be discussed.

EXPERIMENTAL

$\text{Zn}_{1-x}\text{Fe}_x\text{Se}$ crystals were grown by the modified Bridgman method, and crystallized in the zinc-blende structure which is similar to ZnSe in the range of Fe composition $0 \leq x \leq 0.30$.¹⁷ Energy-dispersive x-ray-diffraction

* Correspondence to: C.-M. Lin, National Hsinchu Teachers' College, Hsinchu, Taiwan, R.O.C.
Contract/grant sponsor: National Science Council, Taiwan; Contract/grant numbers: NSC88-2112-M-134-001; NSC87-2112-M-009-009.

(EDXD) measurement has been employed to characterize the structure phase of $\text{Zn}_{1-x}\text{Fe}_x\text{Se}$ crystals at ambient pressure. The source of EDXD is the superconductor wiggler synchrotron beam line X17C of the National Synchrotron Light Source (NSLS) of Brookhaven National Laboratory, U.S.A. Figure 1 shows the EDXD pattern of the $\text{Zn}_{1-x}\text{Fe}_x\text{Se}$ samples. One can note from Fig. 1 that the composition of the $\text{Zn}_{1-x}\text{Fe}_x\text{Se}$ samples is homogeneous. In Fig. 1, the B3 (zinc-blende) phase but not the wurtzite phase can be observed. Our samples were then ground to 1 μm size for micro-Raman measurement. The crystals and ruby chips were sealed with the pressure transmitting medium (deionized water) in the sample chamber which is a hole of 165 μm diameter and 50 μm deep drilled in the stainless steel 301 gasket as used in the previous works.⁸ The pressure was calibrated by the fluorescence scale method.^{18,19} In each run, the applied pressure was homogeneous by using the pressure value which was obtained from averaging the values determined from four ruby chips in the sample chamber. Ruby fluorescence and Raman scattering measurements were performed in a Renishaw 2000 micro-Raman system. The 5145 radiation with power of 0.6 W from the Coherent INNOVA 5.0 W Argon ion laser was focused to about 5 μm on the sample surface. Most of the laser power is lost on the way and only 10% of the intensity reaches the sample. The back-scattered signal was collected by a microscopic system and recorded with a Peltier cooled CCD detector. The recording time for each ruby fluorescence was of the order of 1 s, and Raman spectrum, 10 min. After the experiments, the spectra were processed under a Peakfit program as in previous work.¹⁰ The precision in the frequency determination was in the range of 1 cm^{-1} . The corresponding error of pressure values was within ± 1.0 GPa at the highest pressure obtained because a good signal-to-noise ratio could be achieved in the system even for broad peaks.

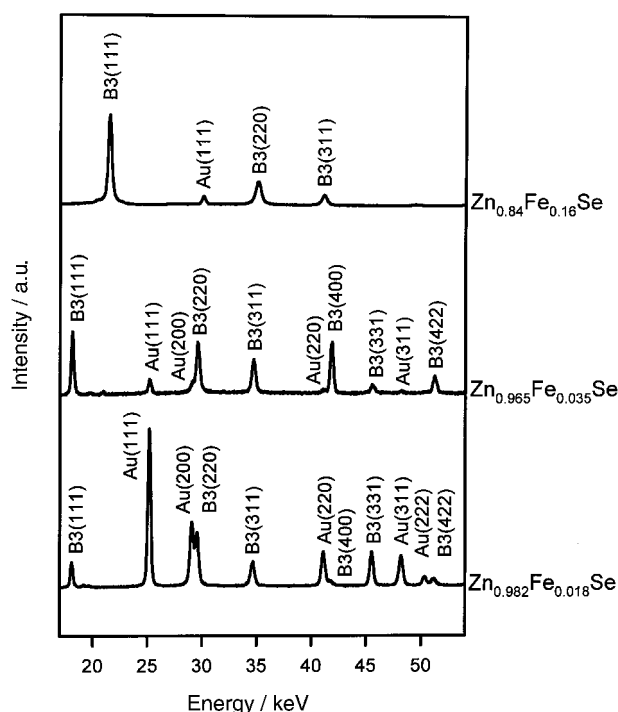


Figure 1. A series of spectra of $\text{Zn}_{1-x}\text{Fe}_x\text{Se}$ at ambient pressure. There is only the B3 (zinc-blende) phase, which also contains the standard identified pressure lines of internal gold.

RESULTS AND DISCUSSION

The pressure dependence of Raman scattering spectroscopy at room temperature for $\text{Zn}_{1-x}\text{Fe}_x\text{Se}$, $x = 0.018$ and 0.035 , is shown in Figs 2 and 3, respectively. Similar results of Raman spectra of ZnSe and $\text{Zn}_{0.84}\text{Fe}_{0.16}\text{Se}$ were reported by Lin *et al.*^{8,10} At atmospheric pressure, two peaks identified as LO and TO phonons were observed at 250 and 200 cm^{-1} , 253 and 206 cm^{-1} for $\text{Zn}_{1-x}\text{Fe}_x\text{Se}$, $x = 0.018$ and 0.035 , respectively, as reported previously.^{8,10,20,21} Between these two peaks, a weak structure attributed to the Fe local (impurity) phonon mode can be labelled through the deconvolution process.^{8,10} The labelled Fe local phonon mode arises from the introduction of the local electric field resulting from the substitution of a Zn atom by an Fe atom.²¹ At around 1.8 and 2.5 GPa, for $x = 0.018$ and 0.035 , the Fe local mode becomes more intense at higher pressure and the Raman shift energy increases with the pressure. The pressure effects on the LO and TO phonon modes exhibit similar blue-shift behaviour as the Fe local phonon mode. Two new phase transitions before metallization occur at 3.3 and 5.9 GPa for $\text{Zn}_{0.982}\text{Fe}_{0.018}\text{Se}$ and 4.5 and 7.2 GPa for $\text{Zn}_{0.965}\text{Fe}_{0.035}\text{Se}$, respectively. This is similar to the case of ZnSe at 4.7 and 9.1 GPa. But for $\text{Zn}_{0.84}\text{Fe}_{0.16}\text{Se}$, two new modes appeared as the pressure was increased to 4.7 GPa.^{8,10} The peaks of Raman phonons located at 204.6 and 208.3 cm^{-1} (labelled as TO split mode I) for $x = 0.018$ and 0.035 exhibited red shift, whilst the peaks of Raman modes located at 220.5 and 225.4 cm^{-1} (labelled as TO split mode II) exhibited blue shift for $x = 0.018$ and 0.035 , respectively. Note that in the recent x-ray work of Greene *et al.*²² on $\text{Zn}_{0.83}\text{Fe}_{0.17}\text{Se}$, an anomaly was also found at a pressure around 5.0 GPa, although no structure transitions were identified by Quadri *et al.*⁴ for pressure lower than 10.0 GPa from the EDXD work. In contrast to the case of $\text{Zn}_{1-x}\text{Fe}_x\text{Se}$, the new phase transitions were ignored in the previous studies of pure ZnSe , although these two phase transitions were reported in the high-pressure Raman study of $\text{Zn}_{1-x}\text{Mn}_x\text{Se}$.⁷ In the case of $\text{Zn}_{1-x}\text{Mn}_x\text{Se}$, one more mode, the Mn impurity mode, was also observed. Arora *et al.*⁶ reported that the splitting of the impurity mode at 4.0 GPa was caused by the lowering of the crystal symmetry. Later, Arora and Sakuntala⁷ found one more phase transition occurred at 8.0 GPa. At 8.0 GPa, the sample became opaque. This transition was considered as a transformation from the direct to indirect band gap. However, if one refers to the study of the similar cubic structure of CdTe ¹⁶ and ZnTe ,^{23,24} more phases (cinnabar and cinnabar and orthorhombic for ZnTe) were found before they underwent the structure transformation from B3 phase to B1 phase. Therefore, we suspect that $\text{Zn}_{1-x}\text{Fe}_x\text{Se}$ might also undergo a similar structure transformation from the B3 through cinnabar and orthorhombic to the B1 structure for $x = 0$, (4.7, 9.1, and 14.4 GPa), 0.018 (3.3, 5.9, and 12.8 GPa), 0.035 (4.5, 7.2, and 12.0 GPa), and 0.16 (4.7 and 10.9 GPa), respectively. As the pressure was increased further to 14.4, 12.8, 12.0, and 10.9 GPa which were the semiconductor–metal transition pressures for $x = 0$, 0.018, 0.035, and 0.16, respectively, both LO and Fe local modes disappeared.¹³ The higher the Fe ion concentration the more the reduction in semiconductor–metal transition pressure value. The disappearance of the LO phonon and Fe local phonon

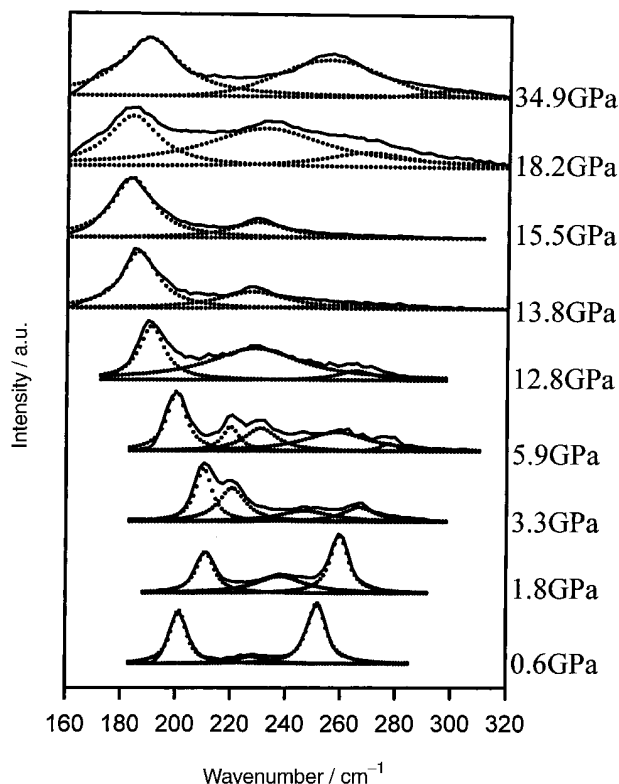


Figure 2. Pressure dependence of phonon wavenumbers of $Zn_{0.982}Fe_{0.018}Se$. Note the lowest frequency component was softened at high pressure and was continuous to 34.9 GPa.

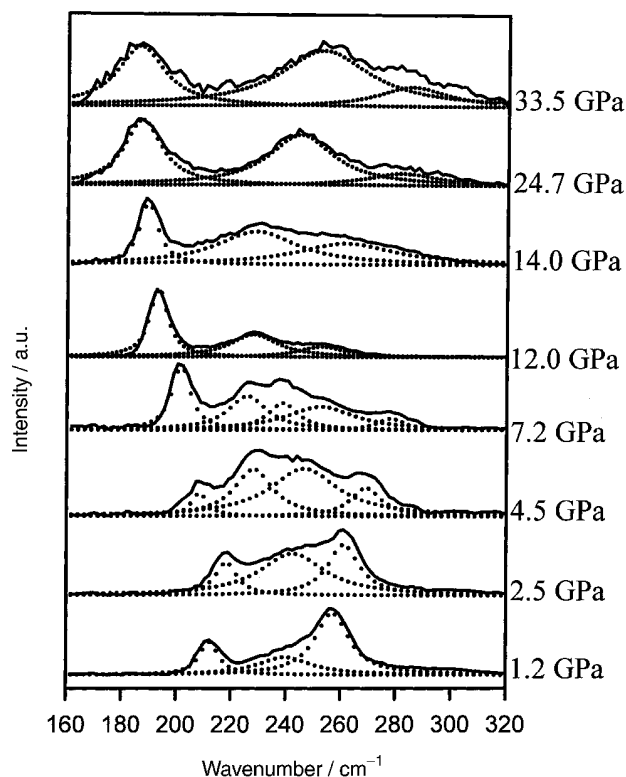


Figure 3. Pressure dependence of phonon wavenumbers of $Zn_{0.965}Fe_{0.035}Se$. Note the lowest frequency component was softened at high pressure and was continuous to 33.5 GPa.

modes can be understood as a semiconductor–metallic transition from the high-pressure resistivity²⁵ and Raman spectroscopy measurements on ZnSe powder.^{8,10} Three

Table 1. Phase transition presents (including those of two new phases) of $Zn_{1-x}Fe_xSe$ are listed and compared with ZnSe

Sample	New phase (I) pressure (GPa): red shift	New phase (II) pressure (GPa): blue shift	Metallization pressure (GPa)
ZnSe	4.7	9.1	14.4
$Zn_{0.982}Fe_{0.018}Se$	3.3	5.9	12.8
$Zn_{0.965}Fe_{0.035}Se$	4.5	7.2	12.0
$Zn_{0.84}Fe_{0.16}Se$	4.7	4.7	10.9

phase transition pressures of $Zn_{1-x}Fe_xSe$ are listed in Table 1.

The variations of Raman mode energies of ZnSe, $Zn_{0.982}Fe_{0.018}Se$, $Zn_{0.965}Fe_{0.035}Se$, and $Zn_{0.84}Fe_{0.16}Se$ as functions of the pressure are shown in Fig. 4. The open, dark shaded, light shaded, and solid symbols correspond to the samples with ZnSe, $Zn_{0.982}Fe_{0.018}Se$, $Zn_{0.965}Fe_{0.035}Se$, and $Zn_{0.84}Fe_{0.16}Se$, respectively. From these plots, one can reconfirm that the phase transition occurred at 14.4, 12.8, 12.0 and 10.9 GPa for ZnSe, $Zn_{0.982}Fe_{0.018}Se$, $Zn_{0.965}Fe_{0.035}Se$, and $Zn_{0.84}Fe_{0.16}Se$, respectively. These phase transitions relate structure transformation from the four-coordinated B3 structure (semiconductor) to a six-coordinated B1 structure (metal). Our results are consistent with the results obtained by Itkin *et al.*¹³ and Greene *et al.*²² The Grüneisen parameter (γ_i) for a quasi-harmonic mode i of frequency, ω_i , the wavenumber in cm^{-1} , was defined by Cadona *et al.*,²⁶ B_0 is the bulk modulus at zero pressure, and is taken as 62.4 GPa²⁷ for all samples.

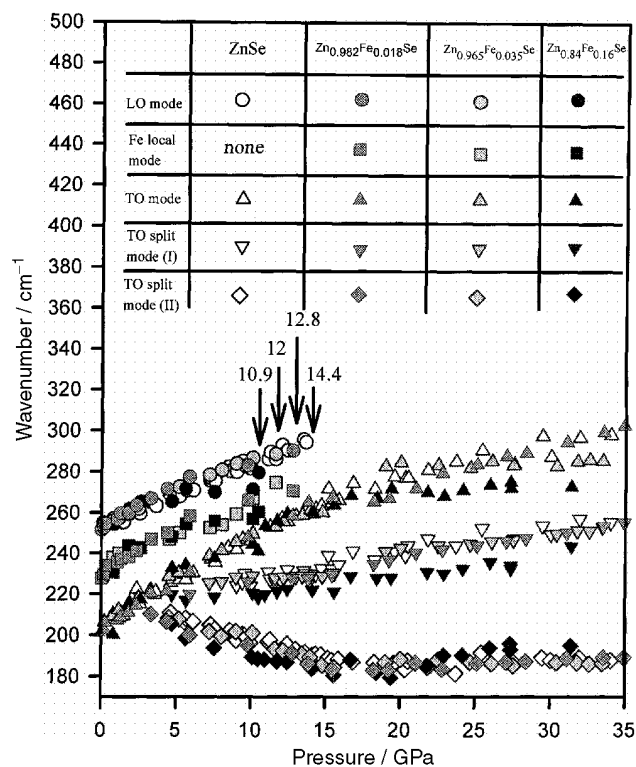


Figure 4. Pressure dependence of Raman peaks in the $Zn_{0.84}Fe_{0.16}Se$ (solid symbols), $Zn_{0.982}Fe_{0.018}Se$ (dark shaded symbols), $Zn_{0.965}Fe_{0.035}Se$ crystals (light shaded symbols) and ZnSe powder (open symbols). The arrows at 10.9, 12.0, 12.8, and 14.4 represent the semiconductor–metal phase transition pressures of $Zn_{0.84}Fe_{0.16}Se$, $Zn_{0.982}Fe_{0.018}Se$, $Zn_{0.965}Fe_{0.035}Se$, and ZnSe, respectively.

Table 2. Effect of pressure on various Raman vibrational modes of $\text{Zn}_{0.982}\text{Fe}_{0.018}\text{Se}$, $\text{Zn}_{0.965}\text{Fe}_{0.035}\text{Se}$, and $\text{Zn}_{0.84}\text{Fe}_{0.16}\text{Se}$, respectively, at room temperature (298K). The values of mode wavenumbers $\tilde{\nu}_i$, pressure dependence ($d\tilde{\nu}_i/dp$), mode Grüneisen parameter γ_i and ($d\gamma_i/dp$) were extrapolated at ambient conditions

Sample	Mode	$\tilde{\nu}_i/\text{cm}^{-1}$	$d\tilde{\nu}_i/dp/\text{cm}^{-1}\text{ GPa}^{-1}$	$\left(\frac{K_0}{\tilde{\nu}_i}\right)\left(\frac{d\tilde{\nu}_i}{dp}\right)$	$d\gamma_i/dp/\text{GPa}^{-1}$
$\text{Zn}_{0.982}\text{Fe}_{0.018}\text{Se}$	LO	252.1	$5.01 - 0.17p$	1.24	$-0.11 + 3.23 \times 10^{-3}p$
	Fe local	222.5	$5.89 - 0.23p$	1.65	$-0.15 + 5.43 \times 10^{-3}p$
	TO	197.2	$5.56 - 0.7p$	1.76	$-0.05 + 1.14 \times 10^{-3}p$
	TO split (I)	209.5	$1.44 - 0.003p$	0.43	$0.0015 - 1.04 \times 10^{-5}p$
	TO split (II)	213.0	$-2.43 + 0.05p$	-0.71	$0.014 + 1.58 \times 10^{-3}p$
$\text{Zn}_{0.965}\text{Fe}_{0.035}\text{Se}$	LO	252.0	$4.35 - 0.199p$	0.91	$-0.064 + 1.66 \times 10^{-3}p$
	Fe local	239.0	$0.9 + 0.324p$	0.23	$0.088 + 2.67 \times 10^{-3}p$
	TO	204.7	$5.43 - 0.181p$	1.65	$-0.08 + 1.49 \times 10^{-3}p$
	TO split (I)	215.4	$1.21 - 0.005p$	0.35	$-0.0033 + 3.02 \times 10^{-5}p$
	TO split (II)	219.5	$-2.79 + 0.11p$	-2.51	$0.03 + 3.66 \times 10^{-4}p$
$\text{Zn}_{0.84}\text{Fe}_{0.16}\text{Se}$	LO	254.4	$3.37 - 0.266p$	0.83	$-0.08 + 1.74 \times 10^{-3}p$
	Fe local	228.3	$6.14 - 0.626p$	1.73	$-0.21 + 8.19 \times 10^{-3}p$
	TO	202.6	$5.60 - 0.222p$	1.73	$-0.10 + 2.4740 \times 10^{-3}p$
	TO split (I)	216.5	$0.15 + 0.042p$	0.04	$-0.0121 + 1.61 \times 10^{-5}p$
	TO split (II)	216.0	$-3.57 + 0.198p$	-1.03	$0.01 + 4.12 \times 10^{-3}p$

The pressure effects on Raman vibrational modes of $\text{Zn}_{1-x}\text{Fe}_x\text{Se}$ at room temperature (298 K) are listed in Table 2, respectively. As a comparison with previous work,²⁰ some conclusions can be drawn: (i) the γ_{LO} values of $\text{Zn}_{0.982}\text{Fe}_{0.018}\text{Se}$, $\text{Zn}_{0.965}\text{Fe}_{0.035}\text{Se}$, and $\text{Zn}_{0.84}\text{Fe}_{0.16}\text{Se}$ are very close to one; (ii) $\gamma_{\text{TO}} > \gamma_{\text{LO}}$ for all systems (for any value of x); (iii) the ratio $\gamma_{\text{TO}}/\gamma_{\text{LO}}$ for $x = 0.16$ is the highest among these three compounds. This shows that $\text{Zn}_{0.84}\text{Fe}_{0.16}\text{Se}$ has higher ionicity than $\text{Zn}_{0.965}\text{Fe}_{0.035}\text{Se}$, $\text{Zn}_{0.982}\text{Fe}_{0.018}\text{Se}$, or ZnSe. The higher ionicity is conjectured to result from the Fe impurity. In Fig. 4, one can also find that the transition pressure of the split TO phonon mode which exhibited blue shift decreased as the impurity concentration was increased. But for the other mode which manifested a red shift, the transition pressure was almost a constant value of 4.7 GPa. One can also note that the TO mode split into three components which were still visible for pressures even up to 35.0 GPa in our work. This was not observed in other previous $\text{Zn}_{1-x}\text{Fe}_x\text{Se}$ work. Furthermore, it is found that the semiconductor–metal transition pressures for $\text{Zn}_{0.982}\text{Fe}_{0.018}\text{Se}$, $\text{Zn}_{0.965}\text{Fe}_{0.035}\text{Se}$, and $\text{Zn}_{0.84}\text{Fe}_{0.16}\text{Se}$ are 12.8, 12.0 and 10.9 GPa, respectively, which are 1.6, 2.4, and 3.5 GPa lower than that of ZnSe, respectively, and the higher the Fe ion concentration the more the reduction in semiconductor–metal transition pressure value. The reduction in the transition pressure is due to the existence of Fe which may result in the hybridization of 3d orbitals into the tetrahedral bonds.⁵ Our result is consistent with the study of pressure-induced phase transition of $\text{Zn}_{0.83}\text{Fe}_{0.17}\text{Se}$ by energy-dispersive x-ray-diffraction measurement.⁴

CONCLUSIONS

High pressure Raman scattering spectroscopy of ZnSe powder, $\text{Zn}_{0.982}\text{Fe}_{0.018}\text{Se}$, $\text{Zn}_{0.965}\text{Fe}_{0.035}\text{Se}$, and $\text{Zn}_{0.84}\text{Fe}_{0.16}\text{Se}$ crystals up to 35.0 GPa has been investigated. The existence of the Fe element was found to result in a reduction in the semiconductor–metal phase transition pressure. The disappearance of the LO and Fe local phonons is attributed to the metallization of the $\text{Zn}_{0.982}\text{Fe}_{0.018}\text{Se}$, $\text{Zn}_{0.965}\text{Fe}_{0.035}\text{Se}$, and $\text{Zn}_{0.84}\text{Fe}_{0.16}\text{Se}$ crystals. Three visible TO phonon splitting components in the $\text{Zn}_{1-x}\text{Fe}_x\text{Se}$ system were observed up to 35.0 GPa. The semiconductor–metal transition pressures for the $\text{Zn}_{0.982}\text{Fe}_{0.018}\text{Se}$, $\text{Zn}_{0.965}\text{Fe}_{0.035}\text{Se}$, and $\text{Zn}_{0.84}\text{Fe}_{0.16}\text{Se}$ are 1.6, 2.4, and 3.5 GPa lower than that of the ZnSe, respectively. It was found that the transition pressure of the blue-shifted TO split mode decreased as the impurity concentration was increased. The calculated Grüneisen parameter implied that $\text{Zn}_{0.84}\text{Fe}_{0.16}\text{Se}$ has higher ionicity than $\text{Zn}_{0.965}\text{Fe}_{0.035}\text{Se}$, $\text{Zn}_{0.982}\text{Fe}_{0.018}\text{Se}$, or ZnSe. The reason for the observation of Raman peaks at pressure above the metallization pressure may be the existence of TO modes in the thin surface of the high-pressure metallic phase as in previous works.⁸

Acknowledgements

We would like to thank Professor W. C. Chou for providing the samples used in this study. This work was supported by the National Science Council, Taiwan by the grant number NSC88-2112-M-134-001 at NHCTC and NSC 87-2112-M-009-009 at NCTU.

REFERENCES

1. C. Benoit à la Guillaume, in *Semimagnetic Semiconductors and Diluted Magnetic Semiconductors*, edited by M. Averous and M. Balkanski, pp. 91, 253. Plenum Press, New York (1991).
2. B. T. Jonker, J. J. Krebs, S. B. Qadri and G. A. Prinz, *Appl. Phys. Lett.* **50**, 848 (1987).
3. A. Twardowski, P. Gold, P. Pernambuco-Wise, J. E. Crow and M. Demianiuk, *Solid State Commun.* **64**, 63 (1987).
4. S. B. Qadri, E. F. Skelton, A. W. Webb, N. Moulton, J. Z. Hu and J. K. Furdyna, *Phys. Rev. B* **45**, 5670 (1992).
5. P. Mahashwaranathan, R. J. Sladek and U. Debska, *Phys. Rev. B* **31**, 5212 (1985).

6. A. K. Arora, E. K. Suh, U. Debska and A. K. Ramdas, *Phys. Rev. B* **37**, 2927 (1988).
7. A. K. Arora and T. Sakuntala, *Phys. Rev. B* **52**, 11052 (1995).
8. C. M. Lin, D. S. Chuu, T. J. Yang, W. C. Chou, J. Xu and E. Huang, *Phys. Rev. B* **55**, 13641 (1997).
9. C. M. Lin, D. S. Chuu, J. Xu, E. Huang, W. C. Chou, J. Z. Hu and J. H. Pei, *Phys. Rev. B* **58**, 16 (1998).
10. C. M. Lin, D. S. Chuu, W. C. Chou, J. Xu, E. Huang, J. Z. Hu and J. H. Pei, *Solid State Commun.* **107**, 217 (1998).
11. W. Andreoni and K. Maschke, *Phys. Rev. B* **22**, 4816 (1980).
12. V. I. Smelyansky and J. S. Tse, *Phys. Rev. B* **52**, 4658 (1995).
13. G. Itkin, G. R. Hearne, E. Sterer and M. P. Pasternak, *Phys. Rev. B* **51**, 3195 (1995).
14. M. Côté, O. Zakharov, A. Rubio and M. L. Cohen, *Phys. Rev. B* **55**, 13025 (1997).
15. R. Ahuji, P. James, O. Eriksson, J. M. Wills and B. Johansson, *Phys. Stat. Sol. (B)* **199**, 75 (1997).
16. R. J. Nelmes, M. I. McMahon, N. G. Wright and D. R. Allan, *Phys. Rev. B* **51**, 15723 (1995).
17. N. Samarth and J. K. Furdyna, *Mat. Res. Soc. Symp. Proc.* **161**, 427 (1990).
18. H. K. Mao, J. Xu and P. M. Bell, *J. Geophys. Res.* **91**, 4673 (1986).
19. J. Xu, H. K. Mao and P. M. Bell, *Acta Physica Sinica*, **36**, 500 (1987).
20. S. S. Mitra, O. Brafman, W. B. Daniels and R. K. Crawford, *Phys. Rev.* **186**, 942 (1969).
21. C. L. Mak, R. Sooryakumar, B. T. Jonker and G. A. Prinz, *Phys. Rev. B* **45**, 3344 (1992).
22. R. G. Greene, H. Luo and A. L. Ruoff, *J. Phys. Chem. Solids* **56**, 521 (1995).
23. M. I. MacMahon and R. J. Nelmes, *J. Phys. Chem. Solids* **56**, 485 (1995).
24. G. D. Lee and J. Ihm, *Phys. Rev. B* **53**, R7622 (1996).
25. A. Jayaraman, *Rev. Mod. Phys.* **55**, 65 (1983).
26. M. Blackman and W. B. Daniels, in *Light Scattering in Solids IV*, edited by M. Cardona and G. Güntherodt, Chapt. 8. Springer Verlag, Berlin (1984).
27. S. Ves, K. Strössner, N. E. Christensen, C. K. Kim and M. Cardona, *Solid State Commun.* **56**, 479 (1985).